Int J Appl Earth Obs Geoinformation 88 (2020) 102067

Contents lists available at ScienceDirect

Int J Appl Earth Obs Geoinformation

journal homepage: www.elsevier.com/locate/jag

An object-based image analysis approach to assess irrigation-water consumption from MODIS products in Ethiopia

Marjolein F.A. Vogels, Steven M. de Jong*, Geert Sterk, Niko Wanders, Marc F.P. Bierkens, Elisabeth A. Addink

Faculty of Geosciences, Utrecht University, POBox80.115 3508 TC Utrecht, the Netherlands

ARTICLE INFO

Keywords:
MODIS product MOD16A2
Rift Valley Ethiopia
Small-holder farming
GEOBIA
Irrigation

ABSTRACT

Efficient water-resource management is essential with regard to food security, growing populations and climate change. This is especially important for low- and middle-income (LMC) countries where food is often locally produced by traditional smallholder farming. Detailed knowledge of the spatio-temporal distribution of irrigation-water consumption provides valuable information to anticipate local food shortages and water scarcity as a result of climate variability. Yet, adequate techniques to quantify irrigation-water consumption at field level over large areas are lacking. Irrigation estimates generally have a coarse resolution making them inadequate for field-level assessments.

This study developed a remote-sensing-based approach to quantify spatio-temporal patterns of irrigation-water consumption at field level using the MODIS evapotranspiration product (MOD16A2) and existing land-use maps on the spatio-temporal distribution of irrigated agriculture. Object-based image analysis was used to establish local evapotranspiration differences between irrigated and rainfed fields on a monthly basis, which are the irrigation-water consumption rates of the irrigated fields. This novel method was applied to a study area in the Central Rift Valley in Ethiopia where smallholder farming is dominant and only a few large-scale farms are present. Comparison with irrigation-water-consumption values of a local irrigation scheme showed that the monthly temporal dynamics were captured quite well, but lower values were calculated compared to the scheme's field data. Comparison with two validated remote-sensing based studies in Africa showed good agreement as irrigation-water-consumption estimates were in the same order of magnitude. Irrigation-water consumption follows the temporal rainfall pattern, i.e. irrigation practices intensify with increased water availability. Surface water is commonly used for irrigation in the study area.

Our study shows that smallholder practices have a lower irrigation-water consumption compared to modern large-scale farms by approximately a factor 3. Irrigation-water consumption in the area is considerable, especially during the dry season. On average 32 % of excess water (precipitation – evapotranspiration) is consumed for irrigation. For smallholder irrigation and large-scale irrigation specifically this is 28 % and 63 % respectively.

The object-based approach presented here is an operational mapping method for field-level irrigation-water-consumption over large areas. MOD16A2 is a global open-source readily-available evapotranspiration product used here although an evapotranspiration product with a higher spatial resolution might be preferred. Our approach can provide irrigation-water-consumption estimates over large areas in data-poor regions, which will increase the understanding of spatio-temporal patterns of smallholder irrigation and provide information to optimize water use.

1. Introduction

For the next 40 years it is estimated that food production should have to increase by 60 % for high-income countries and by 100 % for low- and middle-income (LMI) countries to safeguard food security (Alexandratos and Bruinsma, 2012). Irrigated agriculture will play a vital role to enhance food production (Smidt et al., 2016; Wu et al., 2018) and irrigation water demands will strongly rise (Deines et al., 2017). Irrigated agriculture is responsible for over 70 % of global freshwater withdrawals (WWAP, 2012). Efficient water-resource management becomes increasingly important given the challenges of food security, growing populations, and climate change (Droogers et al.,

* Corresponding author.
E-mail address: s.m.dejong@uu.nl (S.M. de Jong).

https://doi.org/10.1016/j.jag.2020.102067
Received 31 October 2019; Received in revised form 31 January 2020; Accepted 4 February 2020
Available online 10 February 2020

2010). Detailed quantitative knowledge on water resources used for irrigation is essential to produce accurate and timely information to ensure food and water security (Deines et al., 2017). Such knowledge allows for the assessment of irrigation-impact on catchment hydrology (Beilicci and Beilicci, 2016), the quantification of anthropogenic impacts on water resources (Wada et al., 2014), and the monitoring and evaluation of investments in irrigation infrastructure (FAO, 2011).

Despite the importance of detailed information on irrigation, data and methods for a field-level quantification of irrigation fluxes over large areas and longer periods are not available. A distinction between irrigation-water use and irrigation-water consumption is made here. Irrigation-water use is the volume of water-resource abstraction for irrigation purposes, also called irrigation-water withdrawal. Irrigation-water consumption is the portion of that abstraction that is actually consumed in the form of evapotranspiration, which in turn consists of plant transpiration, soil evaporation and evaporation losses during transport and application. The difference between irrigation-water use and irrigation-water consumption are called return flows. The latter is affected by the efficiency of the irrigation system, which is primarily determined by conveyance losses along irrigation channels and over-irrigation (Perry et al., 2009; Reinders et al., 2013). The relation between irrigation-water use and irrigation-water consumption is defined by FAO (2011) as follows:

$$\text{Irrigation water consumption} = \text{Irrigation efficiency (\%)} \times \text{Irrigation-water use} \quad (1)$$

Measured water withdrawals, e.g. by flow meters or a stage-discharge relationship, provide information on local irrigation-water use, but such approaches are infeasible for large-scale irrigation monitoring as it is labour-intensive and expensive (Van Eekelen et al., 2015). Moreover, the accessibility of such data is often hindered by political issues, especially for transboundary river basins (Awulachew et al., 2012) and a continuous spatio-temporal specification of irrigation is absent (Deines et al., 2017).

Remote sensing can provide spatio-temporal patterns of irrigation-related indicators. Increased soil moisture and increased evapotranspiration are observed as a result of an increase in any available water source (rainfall, irrigation, capillary rise, change in soil moisture), and are highly influenced by cultivation practices (Bastiaanssen and Steduto, 2017). Several studies exploited remote-sensing-derived evapotranspiration estimates for the quantification of irrigation, which generally deploy surface-energy balance algorithms using optical and thermal sensors (Droogers et al., 2010; Mu et al., 2011; Van Dijk et al., 2018; Van Eekelen et al., 2015). Often detailed information on soil, crop types, sowing/harvesting dates, and irrigation practices (timing and duration) are required (e.g. Droogers et al., 2010). Moreover, a temporal specification (e.g. seasonal) at detailed spatial level is generally absent (Deines et al., 2017). Next to optical/thermal sensors to derive evapotranspiration estimates, microwave sensors can be deployed to determine soil moisture and quantify irrigation (Brocca et al., 2018; Kumar et al., 2015). However, these products generally have a very coarse resolution, e.g. Brocca et al. (2018) used radar-derived soil moisture data at around 25 km spatial resolution to quantify irrigation. New developments such as the NASA-EcoStress initiative will yield high resolution 30 by 30 m evapotranspiration products for selected target sites, for now, in the USA (Anderson, 2018). EcoStress (ECOsystem Spaceborne Thermal Radiometer Experiment on Space Station) produces evapotranspiration, evaporative stress and water use efficiency products by measuring the thermal infrared brightness temperatures, in six thermal spectral bands, of plants and using that information to derive evapotranspiration (Meerdink et al., 2019; NASA, 2019; Anderson, 2018). Ecostress was launched in June 2018 and data are becoming available now. So far, existing remote-sensing-based methods on the quantification of irrigation are either highly ground-data dependent or have a very coarse resolution with respect to field-level monitoring. Moreover, it is a laborious and technical task to determine soil moisture or evapotranspiration over large areas from remote-sensing datasets and large-scale open-source availability of such products is rare. Currently, MOD16A2 is the only global readily-available open-source evapotranspiration product providing real-time evapotranspiration estimates (Mu et al., 2007, 2011).

The available tools to quantify spatio-temporal patterns of irrigation are especially impractical and inadequate for the extremely data-poor LMI-countries. These countries are characterized by fragmented and complex agricultural landscapes, due to the small cultivated fields (≤ 1 ha) with inter- or mixed cropping systems (Abate et al., 2000). Next, cultivation has dynamic spatio-temporal patterns of sowing, harvesting and irrigation as planting schedules and water availability for irrigation follow rainfall patterns (Hansen et al., 2011; Vogels et al., 2019), which differ between seasons and years. Food in LMI-countries is mainly produced by traditional-smallholder farming systems (Funk et al., 2009). Following the definition by FAO (2004) we define smallholders as farmers with limited resource endowments and cultivating less than 1 ha of land but forming the backbone of African agriculture and food security for many areas. Frequent food and water shortages occur as a result of climate variability (Wani et al., 2009). Smallholders mainly exploit surface water for irrigation through river diversions and farm dams (USGS, 2016; Siebert et al., 2013; Lebdi, 2016), which is generally unregulated and not registered. Food-security-policy frameworks focus on smallholder irrigation development to enhance food production (Beekman et al., 2014). Tools to identify and quantify smallholder irrigation at field level over large areas are valuable in this context. Unfortunately, these data-poor complex agricultural landscapes complicate irrigation mapping (Ozdogan et al., 2010; Bégué et al., 2018). Furthermore, existing, regional to global, water-balance studies do not incorporate smallholder irrigation (e.g. Siebert and Döll, 2010; Wada et al., 2014), as detailed information is absent. Water-resource planning for smallholder-dominated areas is currently not possible and the impact of smallholder irrigation on the water balance remains uncertain.

The aim of this study is to develop a completely remote-sensing based approach to quantify monthly irrigation-water consumption at field level using Geographic Object-Based Image Analysis (GEOBIA) and the MODIS evapotranspiration product MOD16A2. Monthly field-level information on the distribution of irrigated and rainfed agriculture is derived from Vogels et al. (2019). Process-based rules are applied to quantify monthly irrigation-water consumption for irrigated fields using the evapotranspiration of neighboring rainfed field as a local baseline. This GEOBIA approach is applied to a case-study area in the Central Rift Valley, Ethiopia. This area is dominantly cultivated by traditional smallholder farming, but also a few large-scale irrigation schemes are present. The research questions of this study are: 1) how can irrigation-water consumption be determined using GEOBIA, 2) what is the irrigation-water consumption in the study area, 3) what are the differences in irrigation-water consumption between traditional smallholder and modern large-scale agriculture, 4) what is the impact of irrigation on the water balance, and 5) what is the applicability of the developed approach.

2. Data and methods

This study specifically quantifies irrigation-water consumption (or IWC) rather than irrigation-water use. It builds on the results of Vogels et al. (2019), who use NDVI time series derived from Sentinel-2 imagery and a GEOBIA workflow to determine the monthly distribution of irrigated agriculture in the Horn of Africa. Three different spatial-heterogeneity thresholds (15 %, 25 %, and 35 %) were used to describe local vegetation development and to discriminate irrigation-induced crop growth from rainfall-induced crop growth. The assumption was that irrigation is applied at field level resulting in vegetation change at the field level, while a rainfall event leads to vegetation changes over

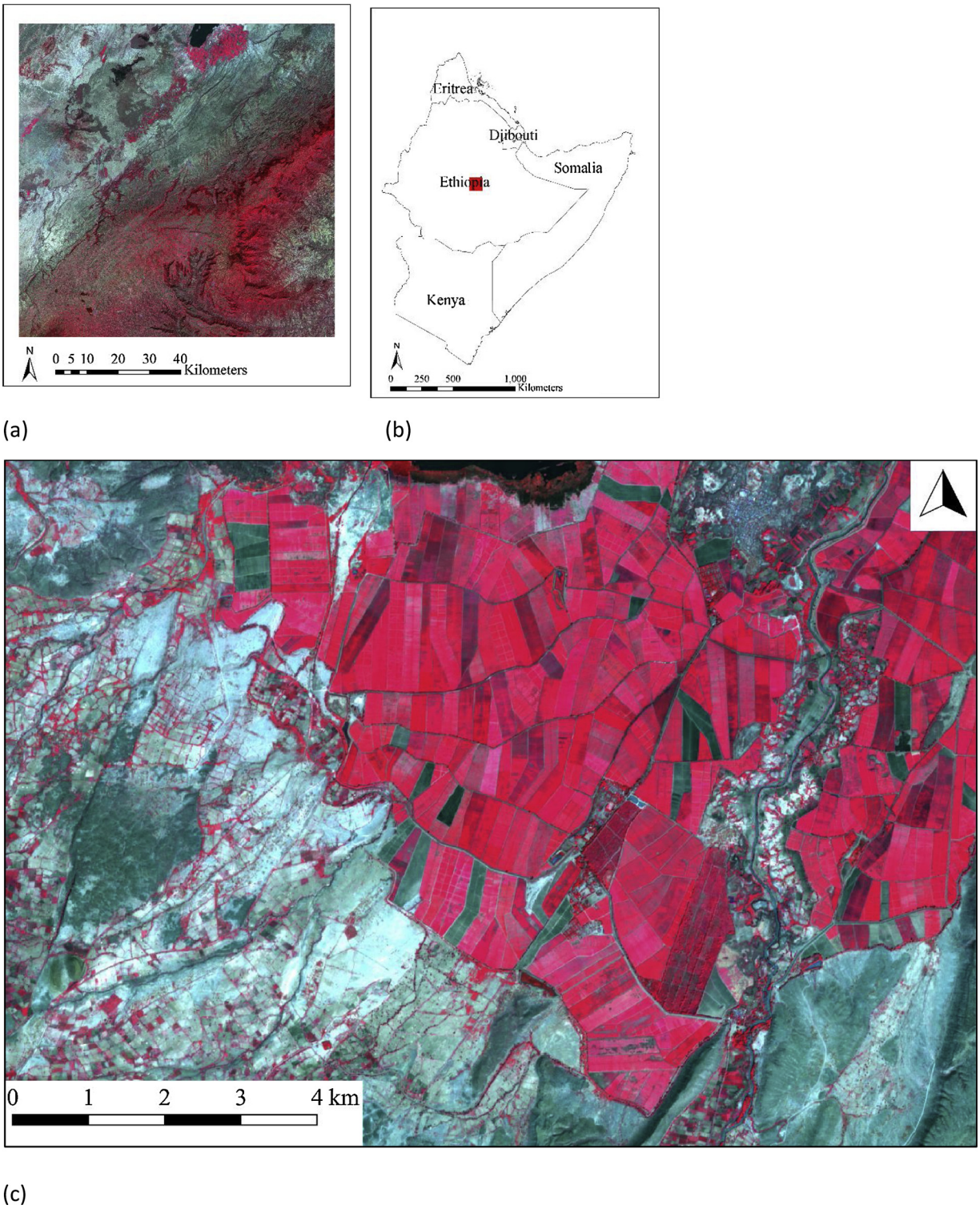

Fig. 1. The location of the study area in the Central Rift Valley, Ethiopia (1a & 1b). F1a shows an area of ~100 × 100 km^2 where large scale agriculture is located in the central north area and smallholder's area in the northwestern corner. 1c shows a subarea witha part of the large-scale Metahara irrigation scheme. Modern large-scale agriculture is located in the central and north-east, smallholder agriculture is located in the south-west part along the Awash River (running from south to north in the east part of the image). Images in 1a and 1c show the best-cloud-free image between May 2018 and December 2018, with RGB: NIR, red, green. Center coordinates of 1a are 8∘24:053′N 39∘48:181′E.

larger areas than the field (similar changes will occur over many fields). For example, if 100 % of the area around a field shows vegetation growth, the vegetation growth of this field is attributed to rainfall. In contrast, if 65 % of the area around a field shows vegetation growth and 35 % (heterogeneity threshold) shows no growth, the vegetation growth is attributed to irrigation. In summary, these heterogeneity thresholds describe cutoffs as to which spatial extent of the area (e.g. 15 %, 25 % or 35 % of the area around the field) has to show no-vegetation-growth in order to attribute vegetation growth of a field to either rainfall or irrigation. The high resolution of Sentinel-2 used, provided

monthly field-level data on the spatial distribution of smallholder irrigation in the Horn of Africa. Data from Vogels et al. (2019) used in the current study comprise: 1) monthly land-use/land-cover (LULC) maps showing the distribution of irrigated and rainfed fields (objects), 2) monthly NDVI composites on which they were based, and 3) the field delineation based on the dry-season mosaic. The field objects will serve as the spatial unit in this study.

The study period runs from September 2016 to August 2017. The study area is located in the Central Rift Valley, Ethiopia (Fig. 1) and has an extent of approximately 100 × 100 km^2 (Vogels et al., 2019). The area is situated in a dry part of Ethiopia and the main sources of irrigation water are the Awash river and groundwater. The area experiences two rainy seasons: March to May and July to September. The dry season runs from October to March. The study area is partly located in the Awash River basin serving water to many smallholder farmers (Dejen, 2014). Fields are typically 1 ha in size and cultivated with crops for domestic use by smallholders. Furrow irrigation is most commonly practiced here, i.e. water is lead through channels into the field. Some modern large-scale irrigation schemes are also present in the area, e.g. the Metahara irrigation scheme.

This study determines irrigation-water consumption of irrigated croplands by comparing their evapotranspiration (ET) with that of nearby rainfed croplands (Fig. 2). Irrigation-water consumption was not calculated for times and locations with cloud cover in the NDVI composites. The LULC maps do not show a classification for these no-data cases. Differences in irrigation-water consumption between traditional smallholder and modern large-scale agriculture were also assessed. Modern large-scale agricultural areas were visually identified in imagery from this study, World Imagery (ESRI, 2018) and Google Maps (Google Maps, 2017) using criteria as size, shape, texture and clustering of the fields. All other croplands were considered traditional smallholder agriculture. The spatial coverage of modern large-scale agriculture in our study area is round 7400 ha and the smallholder's area covers around 560.000 ha. To determine the impact of irrigation on available water resources, a simple water balance was adopted.

2.1. Data collection and preprocessing

Two products were used in this study: 1) terra net actual ET 8-day (mm/8-day) from MODIS (MOD16A2) at 500-m spatial resolution (USGS, 2019), and 2) daily precipitation (P in mm/day) from the Climate Hazards Centre InfraRed Precipitation with Station data (CHIRPS, 2019) at approximately 5-km spatial resolution (Fig. 3). Both datasets were selected, because they are readily-available with global coverage and have a high spatio-temporal resolution.

Data collection and preprocessing was done in the Google Earth Engine (Google Earth Engine Team, 2017). Monthly ET was computed from the 8-day ET (USGS, 2019). A higher spatial resolution than 500-m is required for field-level analysis, which was attained by downscaling. The monthly NDVI composites at 10-m resolution from Vogels et al. (2019) were used for this purpose (Fig. 3). Here, the assumption is made that higher NDVI, i.e. more active and healthier vegetation, leads to higher ET. Spatial patterns of MODIS ET correlate well with MODIS net primary production (Mu et al., 2007). All NDVI values below zero were set to zero thereby generating adapted NDVI maps ranging from 0 to 1. Per MODIS pixel, the total NDVI was determined i.e. the sum of all NDVI values. Next, the fraction NDVI was determined at 10-m resolution, which is the NDVI value in a 10-m pixel divided by the total NDVI in a MODIS pixel. Assuming a linear relationship between NDVI and ET, this fraction was then multiplied by the total ET in a MODIS pixel. This downscaling scheme ensures that the sum of the downscaled ET equals the total ET of each MODIS pixel. In this manner monthly 500-m MODIS ET was linearly resampled to 10 m using the NDVI composites (Fig. 3). Daily precipitation was also aggregated to monthly precipitation (Fig. 3). Finally, for each object in the field delineation, monthly ET and monthly precipitation were calculated.

2.2. Quantification of irrigation-water consumption

The spatial units for the irrigation-water-consumption calculations are the irrigated-cropland and rainfed-cropland objects of the LULC maps. These will be further referred to as fields. Irrigation-water consumption is defined as the portion of ET that is related to the application of irrigation. To determine irrigation-water consumption, a baseline ET was established, which represents the ET for rainfed crops. This study assumes that the baseline for a certain irrigated field can be derived from the ET of its nearby rainfed fields. For each irrigated field, the baseline ET was derived from the weighted average ET (thereby correcting for field size) of rainfed neighbors in a radius of 5 km. Then, irrigation-water consumption was calculated by subtracting the baseline ET from the ET of the irrigated field (Fig. 2). This was done on a monthly basis, resulting in monthly maps of irrigation-water

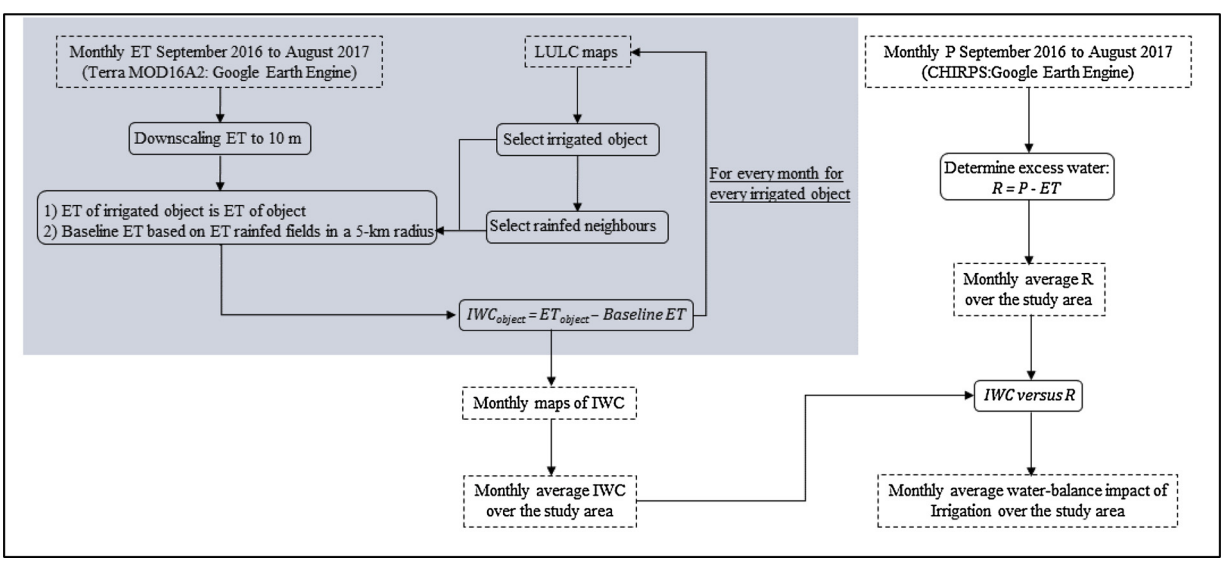

Fig. 2. Workflow of the quantification of irrigation-water consumption (grey block) and the impact on the water balance for the study area. The water-balance components were assessed over the study area as a whole by averaging the water-balance components over the study area (no spatial information) with a specification for modern large-scale agriculture and traditional smallholder agriculture.

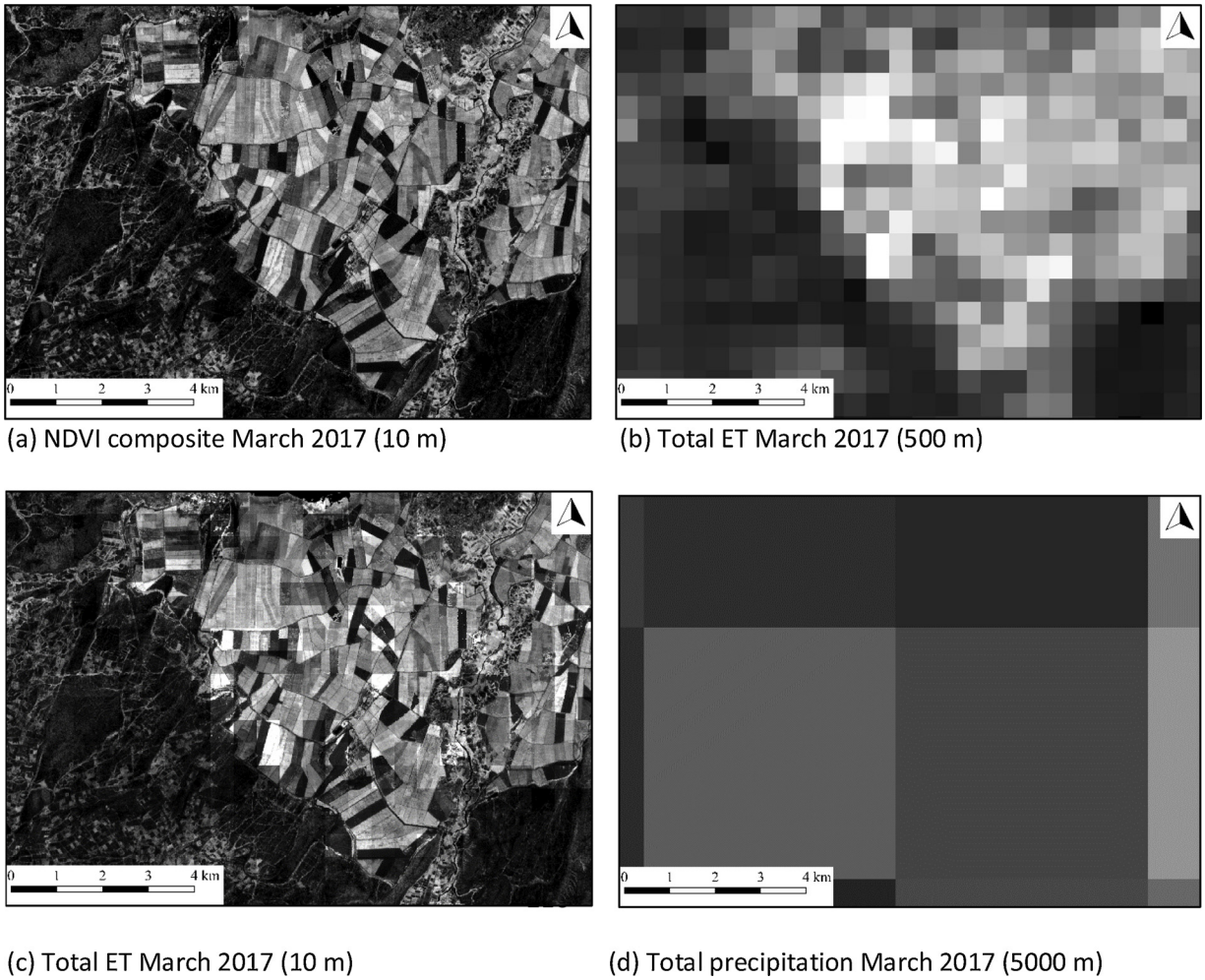

Fig. 3. Illustration of datasets and preprocessing for a small subset area. Monthly 10-m NDVI (a) was used to linearly resample monthly 500-m ET in mm/month (b) to monthly 10-m ET (c). NDVI and ET-Values range from low (dark) to high (bright). Ranges for b and c are similar. Daily 5000-m precipitation in mm/day was also aggregated to monthly precipitation (d).

consumption. ET differences between crop types was not assessed as the remote-sensing based LULC maps differentiate only between agricultural land and other land cover. ET associated with irrigated fields versus ET associated with rainfed fields differed significantly (irrigated ET > rainfed ET) in the study area (t-test: $p < 0.05$).

The time steps of the LULC maps differ between those of the ET and P maps. The LULC maps (Vogels et al., 2019) assessed irrigated agriculture based on differences between months resulting in, e.g. a September - October LULC map. The ET and P maps provide monthly information, e.g. September. Therefore, the LULC maps were transformed to the time steps of the ET and P maps. Details on the temporal matching and transformation of the products is given together with examples in Supplementary Information S1. Only rainfed neighboring fields that were classified as rainfed in two subsequent LULC time steps covering a particular month were incorporated in the baseline calculation.

2.3. Quantification of irrigation-water-consumption impact on the water balance

The straightforward water balance adopted in this study to assess available irrigation water is:

$$R = P - ET \tag{2}$$

Here, P is precipitation, ET is baseline evapotranspiration and R is excess water or recharge, the part of precipitation that is not directly returned to the atmosphere by evapotranspiration. The recharge can be positive or negative depending on the ratio between precipitation and evapotranspiration. If positive, it consists of runoff, soil moisture increase and deep percolation, if negative it consists of soil moisture decrease only. Irrigated agriculture in LMI-countries dominantly uses surface water for irrigation purposes. This excess water will be used as an indicator of water availability for irrigation to assess the impact of irrigation on available water resources. Putting monthly irrigation-water-consumption values next to monthly excess-water values will give insight on the impact of smallholder irrigation on available water resources. Note that this approach does not account for water losses to deep groundwater aquifers as a results of deep percolation. A further limitation is that excess water from previous months is not considered available for the next months, while this is likely the case. We assume that the losses due to deeper percolation of water are negligible compared to the fraction of water that will drain into the nearby surface water bodies and streams. Lastly, water can enter the study area from outside its borders, e.g. through the Awash River, which is not accounted for.

To evaluate irrigation-water consumption and other water-balance components in the study area as a whole and per-type of agriculture (traditional smallholder versus modern large-scale agriculture), the components (total mm/month) were averaged over the specific area's in order to reduce the impact of clouds (masked pixels).

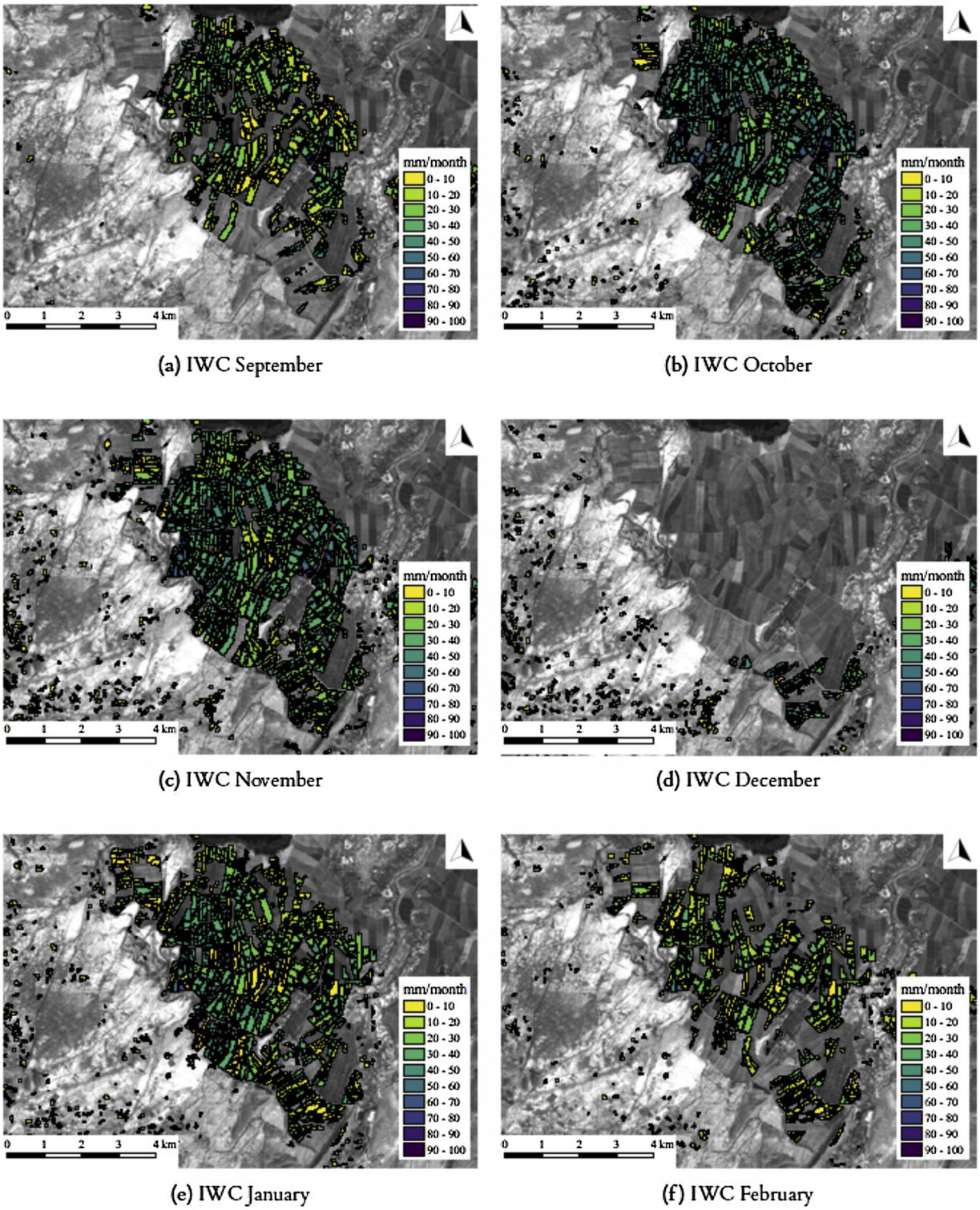

Fig. 4. Spatio-temporal patterns of irrigation-water consumption (LULC map with 15 % threshold is used) for a small part of the Metahara irrigation scheme and surrounding smallholder croplands (Fig. 1c). The black-and-white background is derived from a false-color image (RGB: NIR, red, green) of the best-cloud-free image between May 2018 and December 2018. Center coordinates: 8∘47.295′ N 39∘51.061′E.

3. Results

3.1. Spatio-temporal patterns of irrigation-water consumption

Irrigation-water consumption (IWC) was mapped at a monthly timestep for one year (September 2016 to August 2017) using process-based rules on ET and neighborhood. The output of this study provides monthly patterns of irrigation-water consumption at the field level. The results for a subarea of the Metahara irrigation scheme show that locally IWC varies for most fields between 0 and 50 mm/month with highest IWC in October and lowest in July and August (Fig. 4).

For the complete study area Fig. 5 shows irrigation-water consumption by the black-dashed line. Lowest values are visible for February and March, and peaks in October, January and August (see also

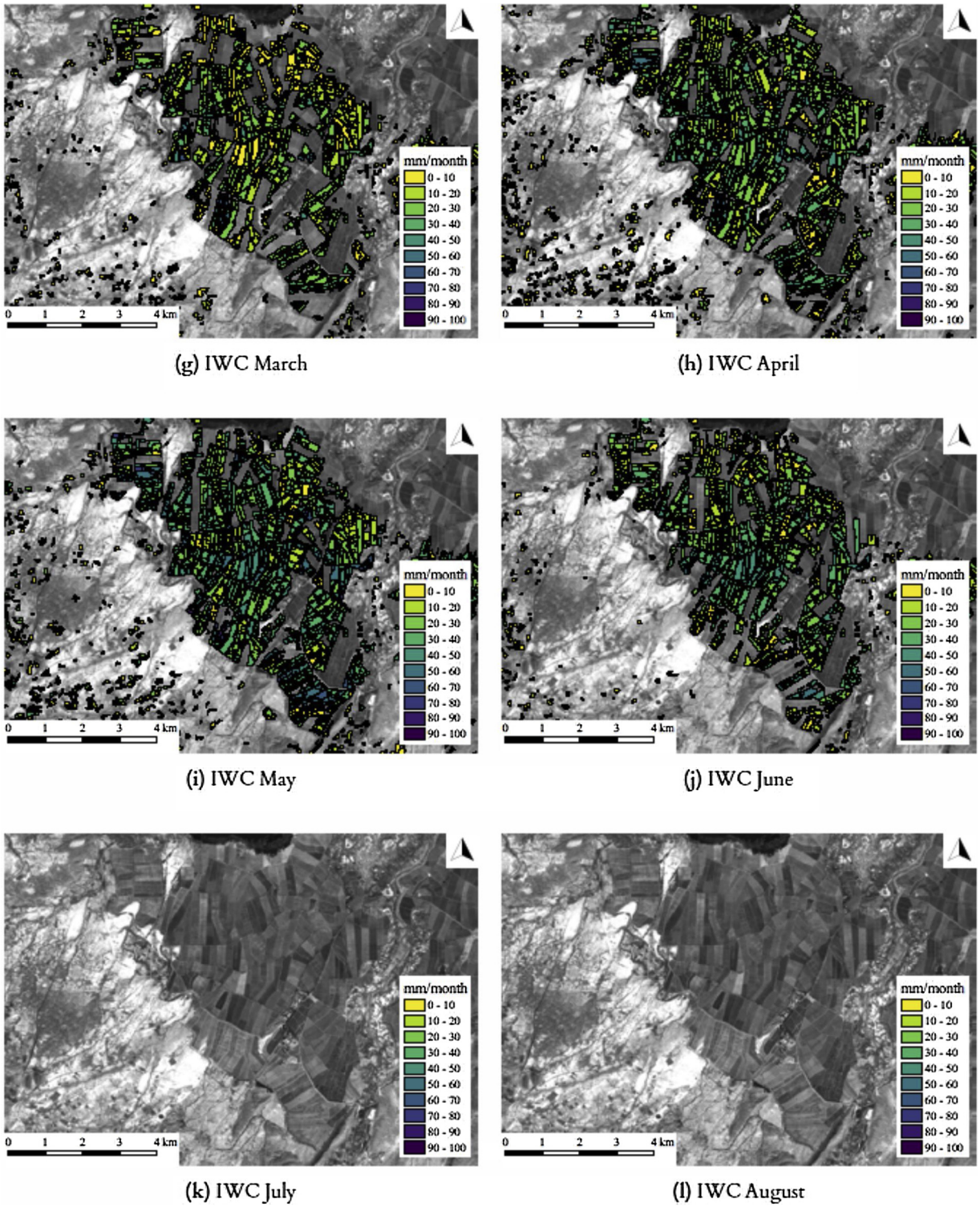

Fig. 4. (*continued*)

Section 3.2). IWC ranges from 4.69 mm/month to 15.52 mm/month (averaged for all thresholds) throughout the studied year. The baseline ET is lowest in January (average of 12 mm/month) and highest in September (average of 62 mm/month). Although considerable differences in mapped irrigated area exist between the three LULC maps (thresholds), these differences are not so pronounced in irrigation-water consumption and baseline ET. The irrigation-water consumption and baseline ET are similar for all thresholds and independent of the irrigated area (Fig. 5).

3.2. Irrigation-water consumption for traditional smallholder agriculture and modern large-scale agriculture

The monthly irrigation-water consumption differs significantly (t-test: $p < 0.05$) between traditional smallholder (~9841 km^2) and modern large-scale agriculture (~209 km^2). The temporal patterns of both types of agriculture resemble (Fig. 6) but the magnitude of irrigation-water consumption is on average a factor 3 higher for modern large-scale agriculture compared to traditional smallholder agriculture.

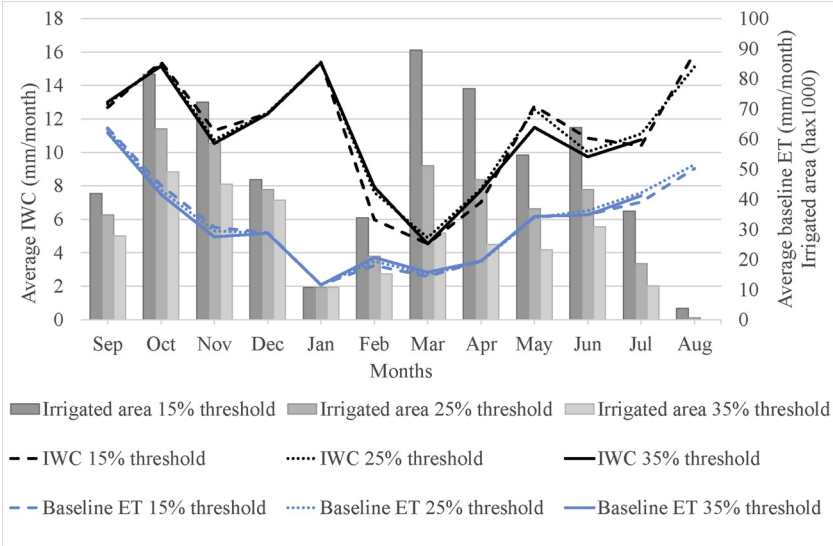

Fig. 5. Temporal irrigation dynamics. Black lines show average irrigation-water consumption by irrigated fields, blue lines show the average baseline ET of rainfed fields and the grey columns indicate the irrigated area. These are all three depicted for the three different LULC maps (three thresholds) of Vogels et al. (2019). Note the double Y-axis on the right for ET and area and the Y-axis on the left for IWC.

Annual total of average monthly irrigation-water-consumption values are 115 mm and 260 mm for smallholder and large-scale agriculture respectively. In August, irrigation-water consumption for modern large-scale agriculture is zero. For the Metahara scheme, Dejen (2014) argues that the assumption is made that rainfall meets the water requirements in this month and that the scheme is partly closed for maintenance. Further inspection of the 15 % LULC map shows that all croplands under modern large-scale agriculture are classified as rainfed agriculture for that month.

3.3. Irrigation-water consumption and the water balance

Precipitation is highest during the two rainy seasons (March - May and July – September: Fig. 7). ET is highest from September to December and from May to August. The lower water availability in the dry season, October to March, clearly lowers ET. Especially July and August have a high availability of excess water throughout the area. From October to January, excess water is negative i.e. there is a rainfall deficit, but considerable water is consumed for irrigation. Highest rainfall deficits occur from October to December. Only during the rainy seasons, irrigation-water consumption is lower than available excess water. Annual totals of average monthly values are 765 mm for precipitation, 420 mm for ET, 415 mm for recharge, 135 mm for irrigation-water consumption, respectively (Fig. 7). For excess water or recharge, only positive values are aggregated over the year. On average 32 % of available excess water is estimated to be consumed for irrigation throughout the year. For smallholders and modern large-scale irrigation these estimates are 28 % and 63 % respectively.

4. Discussion

4.1. Spatio-temporal mapping of irrigation-water consumption

Irrigated agriculture is a highly spatio-temporal dynamic land-use type, which is challenging for mapping (Bégué et al., 2018). Field-level mapping of irrigated agriculture is especially difficult for small cultivated plots with intercropping systems and complex and variable patterns with respect to planting and irrigation, which is characteristic for smallholders in LMI-countries. Vogels et al. (2019) developed a GEOBIA approach to detect irrigated agriculture in such landscapes using Sentinel-2 imagery. This resulted in monthly LULC maps showing the distribution of rainfed and irrigated fields. This follow-up study developed a completely remote-sensing based GEOBIA approach to quantify spatio-temporal patterns of irrigation-water consumption at field level for these irrigated fields. A smallholder-dominated complex agricultural landscape served as a case-study area covering approximately

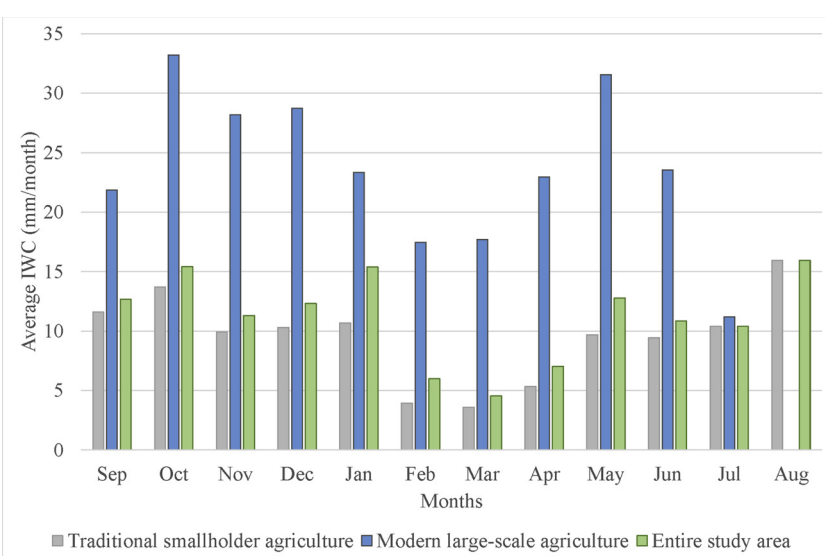

Fig. 6. Differences in irrigation-water consumption for traditional smallholder agriculture and modern large-scale agriculture (LULC map with 15 % threshold is used). The average irrigation-water consumption of the entire study area is also depicted (see Fig. 5), which is closer to the irrigation-water consumption of traditional smallholder agriculture as the area is dominated by smallholder farming.

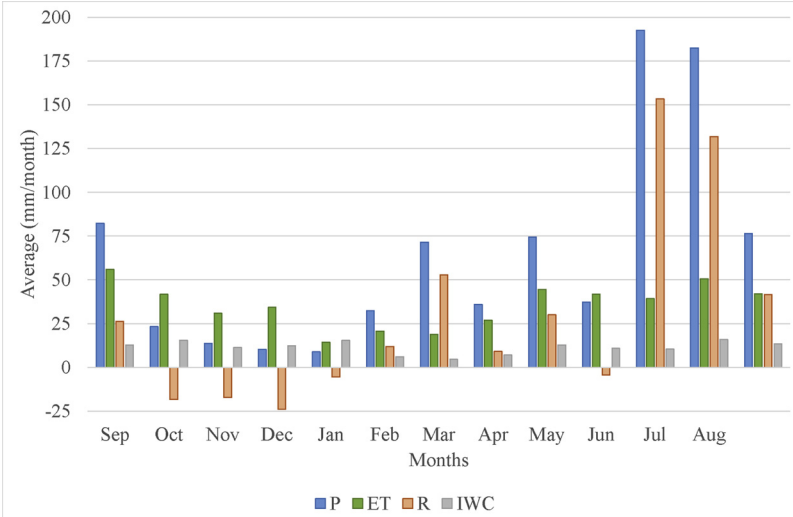

Fig. 7. Overview of different monthly water-balance components for the entire study area (LULC map with 15 % threshold is used). P is precipitation, ET is evapotranspiration, R is excess water and IWC is irrigation water consumption. Note: the irrigation-water consumption values here are the same as the' IWC 15 % threshold' values of Fig. 5.

100×100 km^2. The monthly resolution of the LULC maps enabled the high temporal resolution mapping of irrigation-water-consumption in the area. Generally, LULC maps of irrigated agriculture do not show the temporal dynamics of irrigation (Deines et al., 2017). The irrigation-water consumption is relatively independent of the LULC maps as the differences between the thresholds are minimal (Fig. 5). The irrigation-water consumption follows the rainfall temporal pattern and is highest in the rainy months and lowest during the dry months. The temporal pattern of irrigation-water consumption and baseline ET are not similar. From November to January baseline ET decreases, which is related to decreasing amounts of rainfall i.e. the beginning of dry season. In contrast, from November to January, irrigation-water consumption shows a strong increase. When baseline ET increases from January onwards, this is matched with a strong decrease in irrigation-water consumption from January to March. In February and March, rainfall increases, which means more water is available for evaporation. Surface water is the dominant source for irrigation in LMI-countries and with increased rainfall, there is an increased surface-water availability facilitating irrigation (Fig. 7). A common perception is that during the rainy season no irrigation is required, but water shortages are often reported as a result of varying rainfall patterns (Dejen, 2014) making irrigation essential for an acceptable yield. The known irrigation schemes in this study area commonly apply furrow irrigation, which exploit surface water (Dejen, 2014). In addition, spate-irrigation systems are present in the area (Steenbergen et al., 2011), which are in operation in the rainy season. These systems depend on the seasonal floods in rivers as a result of rainfall.

4.2. Comparison with water-estimated consumption rates of the Metahara irrigation scheme and other remote-sensing-based estimates of irrigation-water consumption

The study area encompasses the Metahara irrigation scheme, which is a modern large-scale irrigation scheme where sugarcane is cultivated (Dejen, 2014). A comparison between the output of this study and estimated irrigation-water consumption rates for the Metahara irrigation scheme was made to evaluate the developed approach with actual field data. Water abstraction from the Awash River was measured for the years 2006–2010 using a stage-discharge relationship at the head reach of the main canal (Fig. 8). These abstraction values were corrected for irrigation efficiency (Dejen, 2014) in order to determine the actual irrigation-water consumption of the crops.

The temporal patterns of irrigation-water consumption of the two products are quite comparable, which indicates that the GEOBIA approach is able to capture temporal irrigation dynamics (Fig. 9). Least irrigation occurs during January to March. Highest irrigation during September to December and May to June. However, irrigation-water-consumption rates of this study are on average only 20 % of the values of Dejen (2014), which can only partly be attributed to different weather conditions between studied years.

Combining irrigation-water consumption from the current study with the irrigation-water use (water-abstraction rates) from Dejen (2014) in equation 1 would result in an average irrigation efficiency of 14 %, which is unrealistically low. The irrigation efficiency to determine the irrigation-water-consumption values of Dejen (2014) was based on the potential ET, which was used to describe the local demand of the crops. Potential ET from Dejen (2014) equals 1325.2 mm/year compared to 2531.8 mm/year as derived from MODIS over the same period, 2006–2010 (Supplementary Information S.2, Table S.1, Column 3 and 4: PET). Olumana et al. (2009) reported a long-term average pan-evaporation rate of 2518.5 mm/year and a reference ET of 1460–2008 mm/year for the Metahara area. Taddese et al. (2010) report a potential ET of 1800 mm/year at Wonji estate, which is a sugarcane estate 50 km from Metahara. This indicates both an overestimation of the irrigation-water consumption according to Dejen (2014) and an underestimation of the values as derived in this study.

Van Dijk et al. (2018) conducted a global remote-sensing-based quantification of irrigation-water consumption by setting up water balances through satellite-data assimilation (2000–2014 at 5-km resolution). The estimates of the resulting water balances were evaluated against river discharge. Irrigation-water-consumption values for Ethiopia have values between ~8–25 mm/month (~100–300 mm/year) and are similar in magnitude as found in the current study. Van Eekelen et al. (2015) conducted a remote-sensing-based quantification of irrigation-water consumption for South Africa, Swaziland and Mozambique (annual total of November 2011 to October 2012) with a detailed land-use map (30-m resolution) and ET estimates derived from SEBAL, which is a surface-energy-balance algorithm (Bastiaanssen et al., 1998). The remote-sensing-derived products were validated against field data (Van Eekelen et al., 2015). For irrigated sugarcane they found irrigation-water consumption values of 33.5 mm/month (402 mm/year) and for irrigated agriculture in general, 20 mm/month (243 mm/year), which are in the same order of magnitude as the results of the current study.

4.3. Differences in irrigation-water consumption between traditional smallholder and modern large-scale agriculture

The irrigation-water consumption differs considerably between traditional smallholder and modern large-scale agriculture in our study

(a) Inlet at Metahara irrigation scheme (b) Main canal downstream of the inlet

Fig. 8. The Awash-River water diversion of the Metahara irrigation scheme (a) and the main channel just downstream of this inlet where water abstraction is measured by the stage-discharge relationship (b).
Source photos: Dejen (2014).

area. Although the coverage of smallholder's areas (~560.000 ha) is much larger than the coverage of large scale agriculture (~7400 ha) in our study area, the number of compared image objects is very large providing a good comparison of the water use between the two types of farming. Irrigation-water consumption of traditional smallholder irrigated agriculture is notably lower (average factor 3) than modern large-scale irrigated agriculture throughout the studied year. Several reasons can explain these differences. It might indicate that smallholders have lower access to irrigation infrastructure and water. Furthermore, large irrigation systems can only persist if they have access to a semi-permanent source of water such as a large stream. Many small-holder schemes may suffer from more intermittent surface-water supply, resulting in less frequent opportunistic irrigation water use. It can also relate to differences in land, crop or water management. The publication of Dejen (2014) about irrigation schemes in the Central Rift Valley in Ethiopia reports irrigation efficiencies of on average 76 % for the Metahara irrigation scheme (modern large-scale agriculture) and 20 % and 40 % for the smallholder irrigation schemes of Golgota and Wedecha respectively. Generally, irrigation schemes in Ethiopia administered by smallholders are poorly managed and are characterized by a low irrigation efficiency due to a lack of knowledge on on-farm water management (Derib et al., 2011; Van Halsema et al., 2011). Regardless of the reasons, it shows a highly unequal distribution of irrigation-water consumption and a higher vulnerability of smallholders to domestic food shortages and water scarcity.

4.4. Impact of irrigation on the water balance

Smallholder irrigation is generally ignored in large-scale water-balance studies (e.g. Siebert and Doll, 2010; Wada et al., 2014). The small-scale nature of this type of agriculture complicates identification and quantification efforts (Ozdogan et al., 2010; Bégué et al., 2018). In Vogels et al. (2019) it was shown that estimates of irrigated area in the Horn of Africa can be up to two times higher than shown in previous LULC-mapping efforts. This reveals that substantial irrigated area and associated water use and consumption is missed if not assessed at the small-scale field level of smallholders. The field-level approach in this study reveals considerable consumption of available excess water for irrigation (Fig. 7). It ranges from 7 to 78 % of available excess water in the rainy season to > 100 % in the dry season, which then shows a high rainfall deficit. On average, 32 % of excess water is used for irrigation-water consumption. Smallholders consume 28 % of available excess water. With the use of a higher-resolution mapping of irrigated agriculture (Vogels et al., 2019), both spatially and temporally, higher estimates of irrigation-water consumption are obtained. Moreover, irrigation efficiency in Ethiopia is relatively low (Derib et al., 2011; Van Halsema et al., 2011), meaning that irrigation-water consumption is much lower than the actual irrigation-water use (withdrawals). If irrigation efficiencies of 30 % are adopted, which is a common irrigation efficiency for Sub-Saharan Africa (FAO, 2011), the impact of irrigation on the water balance is three times higher than the calculated irrigation-water-consumption values (equation 1). However, it should be

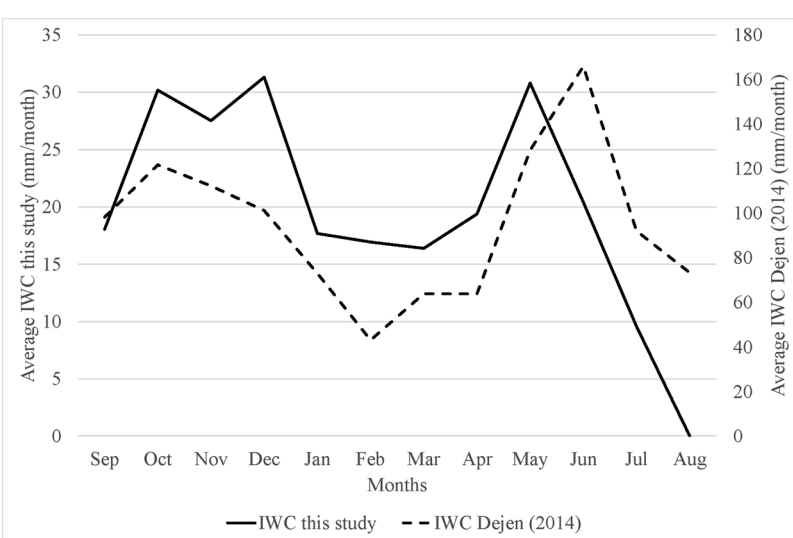

Fig. 9. Comparison of irrigation-water consumption of the Metahara irrigation scheme of this study (LULC map with 15 % threshold is used) and Dejen (2014). Monthly water-abstraction rates from the Awash River were determined by a stage-discharge relationship for the year 2006–2010. Diversion exceeds demand by on average 24 % (Dejen, 2014) and this irrigation efficiency is used to calculate irrigation-water consumption. Note the different scales on the y-axes.

noted that a simplified water balance is used and the calculated water availability (excess water) does not account for infiltration losses, i.e. all excess water is available for irrigation here. On the other hand, water availability for irrigation can be much higher as water can enter the study area from outside its borders, e.g. through the Awash River. Regardless, these findings show that smallholder irrigation has a considerable impact on available water resources, which will affect regional downstream water availability. Smallholder irrigation should be given more attention in future catchment-hydrology studies now tools are available to identify and monitor spatio-temporal patterns of smallholder irrigated agriculture as presented in Vogels et al. (2019) and irrigation-water consumption in this study.

4.5. Applicability of the approach to estimate irrigation-water consumption

The understanding of spatio-temporal distributions of smallholder irrigation is vital information for food- and water-security frameworks. Especially since food shortages and water stress are expected to exacerbate under growing populations and climate change (Brocca et al., 2018). Land productivity of smallholder irrigation in Ethiopia is three times higher than surrounding rainfed farms (Dejen, 2014), so it pays off to invest in irrigation. International development policies focus on the expansion and improvement of smallholder irrigation to improve food security (IAC, 2004; World Bank, 2008; Tschirley, 2011; Burney and Naylor, 2012; United Nations, 2012). Tools to identify and quantify smallholder irrigation occurrence and water use are valuable for monitoring the effectiveness of investment and improvement policies. However, existing tools are hampered by the low data availability and complex agricultural landscapes in LMI-countries. The approach developed in this study is entirely remote-sensing based and does not require extensive knowledge on irrigation practices in the area nor on crop type, planting/harvesting dates or land management. Additionally, it incorporates smallholder irrigated agriculture rather than just large-scale irrigation schemes, the general focus of many irrigation-mapping studies (Abuzar et al., 2015). It enables spatio-temporal quantification of irrigation-water consumption at field level over large areas. Spatio-temporal irrigation-water-consumption information can aid in the assessment of water use and irrigation efficiency and may help to identify areas with potential food and water shortages. The developed approach will provide a basis to optimize water management in existing smallholder irrigation schemes and can aid in a catchment-scale efficient water-resource management.

The LULC maps used in this study provide a minimum estimate of irrigated agriculture (Vogels et al., 2019). The presence of clouds and associated masked pixels in the LULC maps inhibit the identification of irrigated agriculture and consequently the quantification of irrigation-water consumption at certain times and locations. Despite the low influence of the different thresholds of the LULC maps on irrigation-water consumption, underestimation of irrigation-water consumption is likely. The different thresholds also result in different spatio-temporal patterns of irrigation. Field delineation can be improved by using a smaller spatial extent (Vogels et al., 2019). In that case objects coincide better with fields resulting in better field estimates. Furthermore, it would be more convenient to use LULC maps providing monthly information on the spatial distribution of irrigated agriculture, e.g. a LULC map for September as opposed to a September - October LULC map.

This study proves the value of GEOBIA in the large-scale quantification of spatio-temporal patterns of irrigation-water consumption. In its current state, this GEOBIA approach employs MODIS ET, which is the only near real-time open-source ET product globally available at this point in time. The linear downscaling of the 500-m ET with 10-m NDVI will induce uncertainties, especially at the smallholder field-level. Furthermore, this approach is invalid for water bodies as these are characterized by an NDVI equal to zero in this study, but naturally have a high evaporation rate. Ke et al. (2017) showed a relatively good performance of downscaled MODIS ET with 30-m Landsat. The R^2 between 1-km spatial-resolution ET and field data was 0.69 for two flux towers. For the 30-m downscaled ET values, this was 0.76 and 0.82 for the two flux towers respectively. Various studies have described the quality of the MOD16A2 product. Queiroga Miranda et al. (2017) compared the MOD16A2 product with evapotranspiration estimates from flux tower eddy covariance and reports correlations of 0.88 for the 8-day product. NASA (2013) claims a correlation of 0.85 with ET observations in 232 watersheds. Validation of average daily ET from the MODIS ET algorithm showed a correlation coefficient of 0.86 over 46 sites (Mu et al., 2011). Regardless, the current presented methodology is independent of which ET product is used and higher-spatial resolution, with a known accuracy (validated), is recommended for smallholder-dominated agricultural areas. Available surface-energy balance algorithms, such as SEBAL (Bastiaanssen et al., 1998), can provide ET at much higher spatial resolution (e.g. derived from Landsat) and show a much better performance compared to MODIS ET over irrigated areas (Al Zayed et al., 2016). However, an intensive workflow must be followed before ET products are available and requires expert knowledge and judgement, while MODIS ET products are worldwide available since early 2001. ET products at this high resolution are currently not readily available at a global scale although Ecostress (Anderson, 2018) may yield a better, high-resolution product in the future. EcoStress will produce evapotranspiration, evaporative stress and water-use efficiency products of plants every 1–7 days by using thermal infrared brightness temperatures (Meerdink et al., 2019; NASA, 2019; Anderson, 2018). Currently, our study, combined with the workflow in Vogels et al. (2019), provides the first field-level assessment of spatio-temporal patterns of smallholder irrigation-water consumption relying purely on open-source readily available remote-sensing products. As such the methodology is promising for application in other regions in the world and may contribute to a better understanding of spatio-temporal dynamics of irrigation, which is especially useful for large smallholder-dominated areas in data-poor regions common in LMI-countries.

5. Conclusions

We presented a method to assess irrigation-water consumption over large areas (e.g. $\sim 100 \times 100$ km^2 as in this study) including smallholder agriculture area, which is completely remote-sensing based and uses a GEOBIA approach enabling per-field estimates. The land-use maps with the spatio-temporal distribution of irrigated agriculture, which were used as input, are also completely remote-sensing based. These maps are created using open-source Sentinel-2 imagery and smart process-based rules to identify irrigated-agricultural land use. Results show that it is feasible to compute spatio-temporal patterns of irrigation-water consumption. Comparison with field data of the Metahara irrigation scheme shows comparable temporal dynamics, but an underestimation of the approach. In contrast, two validated remote-sensing based approaches in Africa displayed irrigation-water-consumption values in the same order of magnitude as the presented methodology. Our results show that irrigation-water consumption of modern large-scale agriculture is much higher than for traditional smallholder farming, which can either be a result of limited or intermittent access of smallholders to irrigation infrastructure and water resources, or of poor irrigation management resulting in inefficient water use. Results also show that 32 % of the annually available excess water is consumed for irrigation purposes in the study area. 63 % and 28 % for modern large-scale irrigated agriculture and smallholder irrigation respectively. Hence, smallholder irrigation should be considered an important factor in future smallholder-dominated catchment-hydrology studies.

This study developed a globally applicable approach to determine irrigation-water consumption from readily-available remote-sensing products. The method has a high potential to be applied in other regions and climates and offers useful information for efficient water-resource management in the framework of food security and water availability.

This is especially valuable for LMI-countries, which are characterized by a low data availability. This approach enables field-level irrigation-water-consumption mapping over large regions with limited data input.

Funding

This research was funded by Climate-KIC (Task ID: ARED0004_2013-1.1-008_p001-06.

CRediT authorship contribution statement

Marjolein F.A. Vogels: Conceptualization, Methodology, Formal analysis, Writing - original draft. **Steven M. de Jong:** Writing - original draft, Writing - review & editing, Supervision. **Geert Sterk:** Writing - review & editing. **Niko Wanders:** Methodology, Writing - review & editing. **Marc F.P. Bierkens:** Writing - review & editing. **Elisabeth A. Addink:** Conceptualization, Methodology, Funding acquisition, Writing - review & editing.

Declaration of Competing Interest

The authors declare that they have no known competing financial interests or personal relationships that could have appeared to influence the work reported in this paper.

Appendix A. Supplementary data

Supplementary material related to this article can be found, in the online version, at doi:https://doi.org/10.1016/j.jag.2020.102067.

References

Abate, T., Van Huis, A., Ampofo, J.K.O., 2000. Pest management strategies in traditional agriculture: an African perspective. Annu. Rev. Entomol. 45, 631–659. https://doi.org/10.1227/01.NEU.0000153927.70897.A2.

Abuzar, M., McAllister, A., Whitfield, D., 2015. Mapping irrigated farmlands using vegetation and thermal thresholds derived from Landsat and ASTER data in an irrigation district of Australia. Photogramm. Eng. Remote Sens. 81, 229–238. https://doi.org/10.14358/PERS.81.3.229.

Al Zayed, I., Elagib, N., Ribbe, L., Heinrich, J., 2016. Satellite-based evapotranspiration over Gezira irrigation scheme, Sudan: a comparative study. Agric. Water Manag. 177, 66–76. https://doi.org/10.1016/j.agwat.2016.06.027.

Alexandratos, N., Bruinsma, J., 2012. World Agriculture Towards 2030/2050: the 2012 Revision, ESA Working Paper no.12-03. http://www.fao.org/economic/esa/esag/en/.

Anderson, M.C., 2018. ECOsystem Spaceborne Thermal Radiometer Experiment on Space Station (ECOSTRESS) Level-3 Evapotranspiration (ET_ALEXI) Algorithm Theoretical Basis Document. JPL Publication D-94646. Available online. https://ecostress.jpl.nasa.gov/downloads/atbd/ECOSTRESS_L3_Evapotranspiration_ATBD_20180321.pdf.

Awulachew, S., Smakhtin, V., Molden, D., Peden, D., 2012. The Nile River Basin: Water, Agriculture, Governance and Livelihoods. Routledge, Oxon, UK.

Bastiaanssen, W.G.M., Steduto, P., 2017. The water productivity score (WPS) at global and regional level: methodology and first results from remote sensing measurements of wheat, rice and maize. Sci. Total Environ. 575, 595–611. https://doi.org/10.1016/j.scitotenv.2016.09.032.

Bastiaanssen, W.G.M., Menenti, M., Feddes, R.A., Holtslag, A.A.M., 1998. A remote sensing surface energy balance algorithm for land (SEBAL): 1. formulation. J. Hydrol. 212–213, 198–212. https://doi.org/10.1016/S0022-1694(98)00253-4.

Beekman, W., Veldwisch, G.J., Bolding, A., 2014. Identifying the potential for irrigation development in Mozambique: capitalizing on the drivers behind farmer-led irrigation expansion. Phys. Chem. Earth 54–63. https://doi.org/10.1016/j.pce.2014.10.002. Parts A/B/C, 76-78.

Bégué, A., Arvor, D., Bellon, B., Betbeder, J., De Abelleyra, D., Ferraz, R.P.D., Lebourgeois, V., Lelong, C., Simões, M., Verón, S.R., 2018. Remote sensing and cropping practices: a review. Remote Sens. 10, 1–32. https://doi.org/10.3390/rs10010099.

Beilicci, E., Beilicci, R., 2016. Irrigation influence on catchment hydrology modelling with advanced hydroinformatic tools. Res. J. Agric. Sci. 48, 10–21.

Brocca, L., Tarpanelli, A., Filippucci, P., Dorigo, W., Zaussinger, F., Gruber, A., Fernández-prieto, D., 2018. How much water is used for irrigation? A new approach exploiting coarse resolution satellite soil moisture products. Int. J. Appl. Earth Obs. Geoinf. 73, 752–766. https://doi.org/10.1016/j.jag.2018.08.023.

Burney, J.A., Naylor, R.L., 2012. Smallholder irrigation as a poverty alleviation tool in Sub-Saharan Africa. World Dev. 40, 110–123. https://doi.org/10.1016/j.worlddev.2011.05.007.

Climate Hazard Centre, 2019. CHIRPS: Rainfall Estimates From Rain Gauge and Satellite Observations. https://www.chc.ucsb.edu/data/chirps#.

Deines, J., Kendall, A., Hyndman, D., 2017. Annual irrigation dynamics in the U.S. Northern High Plains derived from Landsat satellite data. Geophys. Res. Lett. 44, 9350–9360. https://doi.org/10.1002/2017GL074071.

Dejen, Z.A., 2014. Hydraulic and Operational Performance of Irrigation System in View of Interventions for Water Saving and Sustainability. Ph.D. thesis. UNESCO-IHE Institute for water education, Delft Available at. http://edepot.wur.nl/328862.

Derib, S.D., Descheemaeker, K., Haileslassie, A., Amede, T., 2011. Irrigation water productivity as affected by water management in a small-scale irrigation scheme in the Blue Nile basin, Ethiopia. Exp. Agric. 47, 39–55. https://doi.org/10.1017/S0014479710000839.

Droogers, P., Immerzeel, W.W., Lorite, I.J., 2010. Estimating actual irrigation application by remotely sensed evapotranspiration observations. Agric. Water Manag. 97, 1351–1359. https://doi.org/10.1016/j.agwat.2010.03.017.

ESRI, 2018. ArcGIS Online Standard Service: World Imagery Collection, Map Server. Maps Throughout This Book Were Created Using ArcGIS R Software by ESRI. ArcGIS R and ArcMapTM Are the Intellectual Property of ESRI and Are Used Herein Under License, Copyright C ESRI. Available online: https://www.arcgis.com/index.html (Accessed on 7 February 2018).

FAO, 2004. Smallholders, Globalization and Policy Analysis. Available at. Agricultural Management, Marketing and Finance Service (AGSF) Occasional Paper 5. http://www.fao.org/3/y5784e/y5784e00.htm#Contents.

FAO, 2011. The State of the World's Land and Water Resources for Food and Agriculture (SOLAW) - Managing Systems at Risk. Food and Agriculture Organization of the United Nations, Rome and Earthscan, London doi:978-1-84971-326-9.

Funk, C.C., Brown, M.E., 2009. Declining global per capita agricultural production and warming oceans threaten food security. Food Secur. 1, 271–289. https://doi.org/10.1007/s12571-009-0026-y.

Google Earth Engine Team, 2017. Google Earth Engine: A Planetary-Scale Geo-Spatial Analysis Platform.

Google Maps. 2017. Available online: https://www.google.nl/maps/place/Metehara (Accessed on 7 June 2018).

Hansen, J.W., Mason, S.J., Sun, L., Tall, A., 2011. Review of seasonal climate forecasting for agriculture in Sub-Saharan Africa. Exp. Agric. 47, 205–240. https://doi.org/10.1017/S0014479710000876.

IAC, 2004. Realizing the Promise and Potential of African Agriculture: Implementation of Recommendations and Action Agenda. InterAcademy Council, Amsterdam, The Netherlands, pp. 294. Available as pdf at: ISBN 90-6984-418-4. http://www.interacademies.org.

Ke, Y., Im, J., Park, S., Gong, H., 2017. Spatiotemporal downscaling approaches for monitoring 8-day 30 m actual evapotranspiration. ISPRS J. Photogramm. Remote. Sens. 126, 79–93. https://doi.org/10.1016/j.isprsjprs.2017.02.006.

Kumar, S.V., Peters-Lidard, C., Santanello, J.A., Reichle, R.H., Draper, C.S., Koster, R.D., Nearing, G., Jasinski, M., 2015. Evaluating the utility of satellite soil moisture retrievals over irrigated areas and the ability of land data assimilation methods to correct for unmodeled processes. Hydrol. Earth Syst. Sci. 19, 4463–4478. https://doi.org/10.5194/hess-19-4463-2015.

Lebdi, F., 2016. Irrigation for Agricultural Transformation. Technical Report African Center for Economic Transformation (ACET) and Japan International Cooperation Agency Research Institute (JICA-RI).

Meerdink, S.K., Hook, S.J., Roberts, D.A., Abbott, E.A., 2019. The ECOSTRESS Spectral Library Version 1.0. Remote Sensing of Environment 230. https://doi.org/10.1016/j.rse.2019.05.015.

Mu, Q., Heinsch, F.A., Zhao, M., Running, S.W., 2007. Development of a global evapotranspiration algorithm based on MODIS and global meteorology data. Remote Sens. Environ. 111, 519–536. https://doi.org/10.1016/j.rse.2006.07.007.

Mu, Q., Zhao, M., Running, S.W., 2011. Improvements to a MODIS global terrestrial evapotranspiration algorithm. Remote Sens. Environ. 115, 1781–1800. https://doi.org/10.1016/j.rse.2011.02.019.

NASA, 2013. MODIS Global Terrestrial Evapotranspiration (ET) Product (MOD16A2) Algorithm Theoretical Basis Document. Available at. https://modis-land.gsfc.nasa.gov.

NASA, 2019. The NASA ECOsystem Spaceborne Thermal Radiometer Experiment on Space Station (ECOSTRESS). Available at. https://speclib.jpl.nasa.gov/.

Olumana, M., Loiskandl, W., Fürst, J., 2009. Effect of Lake Basaka expansion on the sustainability of Matahara SE in the Awash river basin, Ethiopia. In: Proceedings of the 34th–WEDC International Conference. Refereed Paper (296). Addis Ababa, Ethiopia. pp. 571–579.

Ozdogan, M., Yang, Y., Allez, G., Cervantes, C., 2010. Remote sensing of irrigated agriculture: opportunities and challenges. Remote Sens. 2, 2274–2304. https://doi.org/10.3390/rs2092274.

Perry, C., Steduto, P., Allen, R.G., Burt, C.M., 2009. Increasing productivity in irrigated agriculture: agronomic constraints and hydrological realities. Agric. Water Manag. 96, 1517–1524. https://doi.org/10.1016/j.agwat.2009.05.005.

Queiroga Miranda, R., Domiciano Galvíncio, J., Soelma Beserra de Moura, M., Jones, C.A., Srinivasan, R., 2017. Reliability of MODIS evapotranspiration products for heterogeneous dry forest: a study case of Caatinga. Adv. Meteorol. 2017. https://doi.org/10.1155/2017/9314801.

Reinders, F.B., Van der Stoep, I., Backeberg, G.R., 2013. Improved efficiency of irrigation water use: a South African framework. Irrig. Drain. 62, 262–272. https://doi.org/10.1002/ird.1742.

Siebert, S., Döll, P., 2010. Quantifying blue and green virtual water contents in global crop production as well as potential production losses without irrigation. J. Hydrol. 384, 198–217. https://doi.org/10.1016/j.jhydrol.2009.07.031.

Siebert, S., Henrich, V., Frenken, K., Burke, J., 2013. Update of the Digital Global Map of Irrigation Areas to Version 5. Technical Report Institute of Crop Science and Resource

Conservation Rheinische Friedrich-Wilhelms-Universität Bonn, Germany.
Smidt, S.J., Haacker, E.M.K., Kendall, A.D., Deines, J.M., Pei, L., Cotterman, K.A., Li, H., Liu, X., Basso, B., Hyndman, D.W., 2016. Complex water management in modern agriculture: trends in the water-energy-food nexus over the High Plains Aquifer. Sci. Total Environ. https://doi.org/10.1016/j.scitotenv.2016.05.127. The, 566-567, 988–1001.
Steenbergen, F.V., Mehari, A., Alemehayu, T., Alamirew, T., Geleta, Y., 2011. Status and potential of spate irrigation in Ethiopia. Water Resour. Manag. 25, 1899–1913. https://doi.org/10.1007/s11269-011-9780-7.
Taddese, G., Sonder, K., Peden, D., 2010. The Water of the Awash River Basin: a Future Challenge to Ethiopia. Available at:. ILRI Working paper: International Livestock Research Institute, Addis Ababa, Ethiopia, pp. 13. www.iwmi.cgiar.org/assessment/files/pdf/publications/WorkingPapers/WaterofAwasBasin.pdf.
Tschirley, D., 2011. What Is the Scope for Horticulture to Drive Smallholder Poverty Reduction in Africa? Policy Synthesis Report No. 88. Available as pdf at. Department of Agriculture, Food and Resource Economics. Michigan State University East Lansing, Michigan. www.agriknowledge.net.
United Nations, 2012. The Future We Want. Resolution Adopted by the General Assembly on 27 July 2012. A/RES/66/288. Technical Report United Nations. .
USGS, 2016. Irrigation Water Use: Surface Irrigation. (Accessed 12 September 2017). https://water.usgs.gov/edu/irfurrow.html.
USGS, 2019. The MODIS/Terra Net Evapotranspiration 8-Day L4 Global 500 M SIN Grid Product: MOD16A2. https://lpdaac.usgs.gov/products/mod16a2v006/.
Van Dijk, A.I.J.M., Schellekens, J., Yebra, M., Beck, H.E., Renzullo, L.J., Weerts, A., Donchyts, G., 2018. Global 5km resolution estimates of secondary evaporation including irrigation through satellite data assimilation. Hydrol. Earth Syst. Sci. 22, 4959–4980. https://doi.org/10.5194/hess-22-4959-2018.
Van Eekelen, M.W., Bastiaanssen, W.G.M., Jarmain, C., Jackson, B., Ferreira, F., Van der Zaag, P., Saraivo Okello, A., Bosch, J., Dye, P., Bastidas-Obando, E., Dost, R., Luxemburg, W., 2015. A novel approach to estimate direct and indirect water withdrawals from satellite measurements: a case study from the Incomati basin. Agric. Ecosyst. Environ. 200, 126–142. https://doi.org/10.1016/j.agee.2014.10.023.
Van Halsema, G.E., Keddi Lencha, B., Assefa, M., Hengsdijk, H., Wesseler, J., 2011. Performance assessment of smallholder irrigation in the central rift valley of Ethiopia. Irrig. Drain. 60, 622–634. https://doi.org/10.1002/ird.613.
Vogels, M.F.A., de Jong, S.M., Sterk, G., Douma, H., Addink, E.A., 2019. Spatio-temporal patterns of smallholder irrigated agriculture in the Horn of Africa using GEOBIA and Sentinel-2 imagery. Remote Sens. 11 (2). https://doi.org/10.3390/rs11020143.
Wada, Y., Wisser, D., Bierkens, M.F.P., 2014. Global modeling of withdrawal, allocation and consumptive use of surface water and groundwater resources. Earth Syst. Dyn. 5, 15–40. https://doi.org/10.5194/esd-5-15-2014.
Wani, S., Sreedevi, T., Rockström, J., Ramakrishna, Y., et al., 2009. Rainfed agriculture – past trends and future prospects. In: Wani, S.P. (Ed.), Rainfed Agriculture: Unlocking the Potential. CAB International, Wallingford.
World Bank, 2008. World Development Report 2008: Agriculture for Development. Washington D.C., USA. https://doi.org/10.1596/978-0-8213-7233-3.
Wu, W., Yu, Q., You, L., Chen, K., Tang, H., Liu, J., 2018. Global cropping intensity gaps: increasing food production without cropland expansion. Land Use Policy 76, 515–525. https://doi.org/10.1016/j.landusepol.2018.02.032.
WWAP, 2012. World Water Assessment Programme. The United Nations World Water Development Report 4: Managing Water under Uncertainty and Risk. 7, place de Fontenoy, 75352 Paris 07 SP, France. 16pp. Available at. United Nations Educational, Scientific and Cultural Organization organizations. https://unesdoc.unesco.org/ark:/48223/pf0000215492.